

Non-invasive Measurements of Cavity Parameters by Use of Squeezed Vacuum

Eugeniy E. Mikhailov, Keisuke Goda, and Nergis Mavalvala
LIGO Laboratory, Massachusetts Institute of Technology, Cambridge, MA 02139, USA

We propose and experimentally demonstrate a method for non-invasive measurements of cavity parameters by injection of squeezed vacuum into an optical cavity. The principle behind this technique is the destruction of the correlation between upper and lower quantum sidebands with respect to the carrier frequency when the squeezed field is incident on the cavity. This method is especially useful for ultrahigh Q cavities, such as whispering gallery mode (WGM) cavities, in which absorption and scattering by light-induced nonlinear processes inhibit precise measurements of the cavity parameters. We show that the linewidth of a test cavity is measured to be $\gamma = 844 \pm 40$ kHz, which agrees with the classically measured linewidth of the cavity within the uncertainty ($\gamma = 856 \pm 34$ kHz).

I. INTRODUCTION

High Q cavities such as whispering gallery mode (WGM) cavities have recently demonstrated quality factors (Q) as high as 2×10^{10} and have shown the potential to reach even higher Q values [1, 2, 3]. However, there are difficulties in measurement of the linewidth and Q of such high Q cavities. While in theory, the Q factor could be as high as 10^{12} and is limited only by Rayleigh scattering [4], in practice, it is limited by other losses in the cavity. They include absorption and scattering losses due to impurities in the cavity material, and light-induced losses due to nonlinear processes. Due to the extremely small mode volume and high Q -factor of the cavity, the cavity build-up intensity is extremely high, even in the case of an input with small power (as small as several mW). Such a high resonator intensity leads to very efficient nonlinear processes inside WGM cavities, such as Raman scattering, second harmonic generation, and four-wave mixing [5]. Whereas this is beneficial in many applications, it causes additional losses in the cavity and thus makes the Q factor measurement unreliable (at least, making it power-dependent) [6].

Squeezed states of vacuum or light have been used in many applications such as improvement in interferometric [7, 8, 9, 10] and absorption [11] measurements, for quantum teleportation [12] and quantum cryptography [13], and for quantum imaging [14]. However, to the best of our knowledge, no experiment for measurements of cavity parameters by use of squeezing has yet been reported. In this paper we propose and demonstrate an alternative method of measuring Q factors by use of a squeezed vacuum field which is equivalent to a field with correlated quantum sidebands [15, 16]. This technique is advantageous over traditional optical methods in that it utilizes the injection of squeezed vacuum into a test cavity not to excite any nonlinear processes in the cavity. When the input field is detuned from the cavity resonance frequency, it transmits only the upper or lower quantum sidebands within the cavity linewidth while reflecting the counterparts (associated upper or lower sidebands) and all the other sidebands. The linewidth of the cavity can then be measured by observing the destruction of the correlation between the upper and lower quantum side-

bands with respect to the carrier frequency. We show that the linewidth and Q factor of a test cavity using the method agrees with those measured by traditional optical methods.

This paper is organized as follows: In Sec. II A, we describe the theoretical framework for the measurement method. In Sec. II B, we explain the validity of the use of squeezed vacuum as a probe for non-invasive measurements and compare the technique to using a classical state. In Sec. III, we demonstrate the method using a test cavity with known cavity parameters and compare the parameter values obtained by the new method and the traditional optical methods. The conclusions of the paper are summarized in Sec. IV.

II. THEORY

A. Destruction of Quantum Sideband Correlation as a Probe for Cavity Parameter Measurements

Consider a squeezed vacuum field with carrier and sideband frequencies, ω_0 and $\omega_0 \pm \Omega$ respectively. As shown in Fig. 1, when the upper sideband of the squeezed vacuum field $a(\omega_0 + \Omega)$ is injected into an optical cavity with resonance frequency ω_c and mirror reflectivities R_1, R_2 , and R_3 , the reflected field $b(\omega_0 + \Omega)$ and its adjoint $b^\dagger(\omega_0 - \Omega)$ are given in terms of $a(\omega_0 + \Omega)$ and its adjoint $a^\dagger(\omega_0 - \Omega)$ by

$$b(\omega_0 + \Omega) = r(\omega_0 + \Omega) a(\omega_0 + \Omega) + l(\omega_0 + \Omega) v(\omega_0 + \Omega), \quad (1)$$

$$b^\dagger(\omega_0 - \Omega) = r^*(\omega_0 - \Omega) a^\dagger(\omega_0 - \Omega) + l^*(\omega_0 - \Omega) v^\dagger(\omega_0 - \Omega), \quad (2)$$

where $r(\omega_0 \pm \Omega)$ is the frequency-dependent cavity reflection coefficient and $l(\omega_0 \pm \Omega)$ is the vacuum noise coupling coefficient associated with transmission and intra-cavity losses. When the cavity is not perfectly mode-matched, the reflected field contains the cavity-coupled reflection a_c [17] and the promptly reflected field a_m that does not

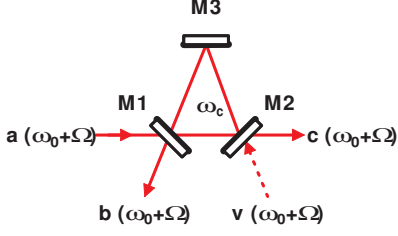


FIG. 1: (Color online) Schematic of a cavity under test. The cavity is composed of three mirrors M1, M2, and M3 in triangular geometry with reflectivities R_1 , R_2 , and R_3 , respectively. a is the upper sideband of an injected field at frequency $\omega_0 + \Omega$, b is the cavity-filtered reflection at the frequency, c is the transmission at the frequency, and v is the vacuum field that couples in due to losses in the cavity at the frequency. ω_c is the cavity resonance frequency. The carrier field at frequency ω_0 transmits through the cavity when $\omega_0 = \omega_c$.

couple to the cavity due to mode mismatch such that

$$r(\omega_0 + \Omega)a(\omega_0 + \Omega) = r_c(\omega_0 + \Omega)a_c(\omega_0 + \Omega) + r_m a_m(\omega_0 + \Omega), \quad (3)$$

$$r^*(\omega_0 - \Omega)a^\dagger(\omega_0 - \Omega) = r_c^*(\omega_0 - \Omega)a_c^\dagger(\omega_0 - \Omega) + r_m^* a_m^\dagger(\omega_0 - \Omega), \quad (4)$$

$$l(\omega_0 + \Omega)v(\omega_0 + \Omega) = l_c(\omega_0 + \Omega)v_c(\omega_0 + \Omega) + l_m v_m(\omega_0 + \Omega), \quad (5)$$

$$l^*(\omega_0 - \Omega)v^\dagger(\omega_0 - \Omega) = l_c^*(\omega_0 - \Omega)v_c^\dagger(\omega_0 - \Omega) + l_m^* v_m^\dagger(\omega_0 - \Omega), \quad (6)$$

where a_c and a_m are spatially orthogonal and

$$r_c(\omega_0 \pm \Omega) = r_c(\omega_d \pm \Omega) = \sqrt{R_1} - \frac{T_1 \sqrt{R_2 R_3} e^{-i[\phi_c(\omega_d) \pm \phi_s(\Omega)]}}{1 - \sqrt{R_1 R_2 R_3} e^{-i[\phi_c(\omega_d) \pm \phi_s(\Omega)]}}, \quad (7)$$

$$r_m = \sqrt{R_1}. \quad (8)$$

Here, ω_d is the detuning from the cavity resonance given by $\omega_d = \omega_0 - \omega_c$ and we have assumed that the resonance frequency of a_m is far from that of a_c such that the reflection coefficient r_m can be treated as a frequency-independent constant at frequencies around the resonance frequency of a_m . The vacuum noise coupling coefficients are then given by

$$l_c(\omega_0 \pm \Omega) = l_c(\omega_d \pm \Omega) = \sqrt{1 - |r_c(\omega_d \pm \Omega)|^2}, \quad (9)$$

$$l_m(\omega_0 \pm \Omega) = l_m(\omega_d \pm \Omega) = \sqrt{1 - r_m^2}. \quad (10)$$

The cavity mirror reflectivity and transmission of each mirror satisfies

$$R_i + T_i + L_i = 1, \quad \text{for } i = 1, 2, 3, \quad (11)$$

where L_i is the loss of each mirror. The intra-cavity losses can be absorbed into R_3 .

Since the carrier is detuned from the cavity resonance frequency, the reflection acquires extra frequency-dependent phase shifts at the detuned carrier frequency

and the sideband frequencies, respectively given by

$$\phi_c = \frac{p}{c} \omega_d = 2\pi \frac{\omega_d}{\omega_{\text{FSR}}}, \quad \phi_s = \frac{p}{c} \Omega = 2\pi \frac{\Omega}{\omega_{\text{FSR}}}, \quad (12)$$

where p and ω_{FSR} are the round-trip length and free spectral range of the cavity, and c is the speed of light in vacuum.

For simplicity, we transform into the rotating frame of the carrier frequency ω_0 in the frequency domain, such that Eqs. (1) and (2) become

$$b(\Omega) = r_c(\omega_d + \Omega)a_c(\Omega) + r_m a_m(\Omega) + l_c(\omega_d + \Omega)v(\Omega) + l_m v_m(\Omega), \quad (13)$$

$$b^\dagger(-\Omega) = r_c^*(\omega_d - \Omega)a_c^\dagger(-\Omega) + r_m^* a_m^\dagger(-\Omega) + l_c^*(\omega_d - \Omega)v^\dagger(-\Omega) + l_m^* v_m^\dagger(-\Omega), \quad (14)$$

where $a_c(\Omega)$ and $a_c^\dagger(-\Omega)$ satisfy the commutation relations

$$[a_c(\pm\Omega), a_c^\dagger(\pm\Omega')] = 2\pi\delta(\Omega - \Omega'), \quad (15)$$

and all others vanish (similarly for $a_m(\Omega)$, $a_m^\dagger(-\Omega)$, $v_c(\Omega)$, $v_c^\dagger(-\Omega)$, $v_m(\Omega)$, and $v_m^\dagger(-\Omega)$). In the two-photon representation [15, 16], the amplitude and phase quadratures of a_c are defined by

$$a_1^c(\Omega) = a_c(\Omega) + a_c^\dagger(-\Omega), \quad (16)$$

$$a_2^c(\Omega) = -i[a_c(\Omega) - a_c^\dagger(-\Omega)], \quad (17)$$

respectively (similarly for a_m , b , v_c , and v_m). A little algebra yields the amplitude and phase quadrature fields of the reflected light in compact matrix form,

$$\mathbf{b} = \mathbf{M}\mathbf{a}_c + r_m \mathbf{a}_m + \mathbf{H}\mathbf{v}_c + l_m \mathbf{v}_m, \quad (18)$$

where we use the two-photon matrix representation

$$\mathbf{a}_c \equiv \begin{pmatrix} a_1^c \\ a_2^c \end{pmatrix} \quad (19)$$

for the operator a_c (similarly for a_m , b , v_c , and v_m),

$$\mathbf{M} = e^{i\varphi_-} \begin{pmatrix} \cos \varphi_+ & -\sin \varphi_+ \\ \sin \varphi_+ & \cos \varphi_+ \end{pmatrix} \begin{pmatrix} A_+ & iA_- \\ -iA_- & A_+ \end{pmatrix} \quad (20)$$

is a matrix representing propagation through the cavity, and

$$\mathbf{H} = \begin{pmatrix} l_+ & il_- \\ -il_- & l_+ \end{pmatrix}. \quad (21)$$

\mathbf{M} comprises an overall phase shift φ_- , rotation by angle φ_+ , and attenuation by factor A_+ . Here we have defined

$$\varphi_\pm \equiv \frac{1}{2} [\arg(r_c(\Omega)) \pm \arg(r_c(-\Omega))], \quad (22)$$

$$A_\pm \equiv \frac{1}{2} [|r_c(\Omega)| \pm |r_c(-\Omega)|], \quad (23)$$

$$l_\pm \equiv \frac{1}{2} [l_c(\omega_d + \Omega) \pm l_c(\omega_d - \Omega)]. \quad (24)$$

In the case of no carrier detuning ($\omega_d = 0$), $r_c(\Omega) = r_c^*(-\Omega)$, and φ_+ and A_- vanish, giving neither quadrature angle rotation nor asymmetrical amplitude attenuation. In the case of cavity detunings ($\omega_d \neq 0$), nonzero φ_+ gives quadrature angle rotation.

From Eq. (18), when we perform homodyne detection of the reflected field with a local oscillator (LO) field, the measured amplitude and phase quadrature variances of the field, defined by $V_1^b = \langle b_1^2 \rangle - \langle b_1 \rangle^2$ and $V_2^b = \langle b_2^2 \rangle - \langle b_2 \rangle^2$ (similarly for $V_1^{a_c}$, $V_2^{a_c}$, $V_1^{a_m}$, and $V_2^{a_m}$), are found in terms of the mode-matched input amplitude and phase quadrature variances $V_1^{a_c}$ and $V_2^{a_c}$ to be

$$\begin{pmatrix} V_1^b \\ V_2^b \end{pmatrix} = \eta_c \begin{pmatrix} \cos^2 \varphi_+ & \sin^2 \varphi_+ \\ \sin^2 \varphi_+ & \cos^2 \varphi_+ \end{pmatrix} \begin{pmatrix} A_+^2 & A_-^2 \\ A_-^2 & A_+^2 \end{pmatrix} \begin{pmatrix} V_1^{a_c} \\ V_2^{a_c} \end{pmatrix} + \eta_m r_m^2 \begin{pmatrix} V_1^{a_m} \\ V_2^{a_m} \end{pmatrix} + \eta_c [1 - (A_+^2 + A_-^2)] \begin{pmatrix} 1 \\ 1 \end{pmatrix} + \eta_m (1 - r_m^2) \begin{pmatrix} 1 \\ 1 \end{pmatrix} + \eta_l \begin{pmatrix} 1 \\ 1 \end{pmatrix}, \quad (25)$$

where η_c and η_m are the composite efficiencies of detection associated with the cavity-coupled and cavity-mismatched modes respectively, η_l is the coupling of detection losses, and $\eta_c + \eta_m + \eta_l = 1$. The detection efficiency is a product of the quantum efficiency of the photodiodes and the mode-overlap efficiency with the LO mode. Eq. (25) can be rewritten in terms of the quadrature variances of the incident field $V_{1,2}^a$ since the cavity-coupled reflection $V_{1,2}^{a_c}$ and the mode-mismatch reflection $V_{1,2}^{a_m}$ originate from the same incident field $V_{1,2}^a$, such that

$$\begin{pmatrix} V_1^{a_c} \\ V_2^{a_c} \end{pmatrix} = \begin{pmatrix} V_1^{a_m} \\ V_2^{a_m} \end{pmatrix} = \begin{pmatrix} V_1^a \\ V_2^a \end{pmatrix}, \quad (26)$$

and therefore,

$$\begin{pmatrix} V_1^b \\ V_2^b \end{pmatrix} = \left[\eta_c \begin{pmatrix} \cos^2 \varphi_+ & \sin^2 \varphi_+ \\ \sin^2 \varphi_+ & \cos^2 \varphi_+ \end{pmatrix} \begin{pmatrix} A_+^2 & A_-^2 \\ A_-^2 & A_+^2 \end{pmatrix} + \eta_m r_m^2 \right] \begin{pmatrix} V_1^a \\ V_2^a \end{pmatrix} + [1 - \eta_c (A_+^2 + A_-^2) - \eta_m r_m^2] \begin{pmatrix} 1 \\ 1 \end{pmatrix}. \quad (27)$$

Note that if the input field is in a vacuum or coherent state such that $V_1^a = V_2^a = 1$, then $V_1^b = V_2^b = 1$, as expected, and no cavity information is contained in the output state b .

If the carrier frequency is detuned downward from the cavity resonance frequency, the cavity transmits only the upper sidebands within the cavity linewidth and replaces them by vacuum at those frequencies while reflecting the associated lower sidebands and all the other sidebands. Hence, the cavity-coupled reflected field is composed of the uncorrelated sidebands within the linewidth and the

reflected correlated sidebands outside of it. The consequence is the destruction of the correlation within the linewidth between the upper and lower quantum sidebands. This is analogous to the destruction of the correlation between electro-optically modulated coherent sidebands in pairs, in which the beat between the carrier and the upper or lower sideband can be measured only when either sideband is absorbed into the cavity, reflecting the carrier and other sideband. The beat could not be observed if all the fields were reflected. Similar measurements could be done with the transmission of the squeezed vacuum field through the cavity. However, the signal-to-noise ratio would not be as good as in the reflection method because the background of the transmission signal is shot noise.

It is convenient to define the test cavity linewidth γ , the quality factor Q , and the finesse \mathcal{F} , as

$$\begin{aligned} \gamma &= \frac{2}{\pi} \omega_{\text{FSR}} \sin^{-1} \left[\frac{1 - \sqrt{R_1 R_2 R_3}}{2(R_1 R_2 R_3)^{1/4}} \right] \\ &\simeq \frac{1 - \sqrt{R_1 R_2 R_3}}{\pi(R_1 R_2 R_3)^{1/4}} \omega_{\text{FSR}}, \end{aligned} \quad (28)$$

$$Q = \frac{\omega_0}{\gamma}, \quad (29)$$

and

$$\mathcal{F} = \frac{\pi(R_1 R_2 R_3)^{1/4}}{1 - \sqrt{R_1 R_2 R_3}} \simeq \frac{\omega_{\text{FSR}}}{\gamma}, \quad (30)$$

respectively. The approximations made in Eqs. (28) and (30) are valid for high Q cavities. R_1 , $R_1 R_2 R_3$, ω_d , and ω_{FSR} will be treated as free fitting parameters. We also assume the input mirror is lossless such that $T_1 = 1 - R_1$.

B. Squeezed/Anti-squeezed Vacuum vs. Classically Noisy Light

Since we are interested in having as little light (at the carrier frequency) as possible in the test cavity, it is instructive to calculate the average photon number in the field we use. The average photon number in squeezed light with squeeze factor r and squeeze angle θ is given by [18]

$$\begin{aligned} \langle N \rangle &= \langle a^\dagger a \rangle \\ &= |\alpha|^2 (\cosh^2 r + \sinh^2 r) - (\alpha^*)^2 e^{i\theta} \sinh r \cosh r \\ &\quad - \alpha^2 e^{-i\theta} \sinh r \cosh r + \sinh^2 r, \end{aligned} \quad (31)$$

where α is the coherent amplitude of the light. As the number of coherent photons becomes zero ($\alpha \rightarrow 0$), resulting in squeezed vacuum, Eq. (31) becomes

$$\langle N \rangle = \langle a^\dagger a \rangle = \sinh^2 r. \quad (32)$$

This is the average photon number in squeezed vacuum generated by squeezing. Note that if the field is unsqueezed ($r = 0$), $\langle N \rangle = 0$. For a squeeze factor of 1.5

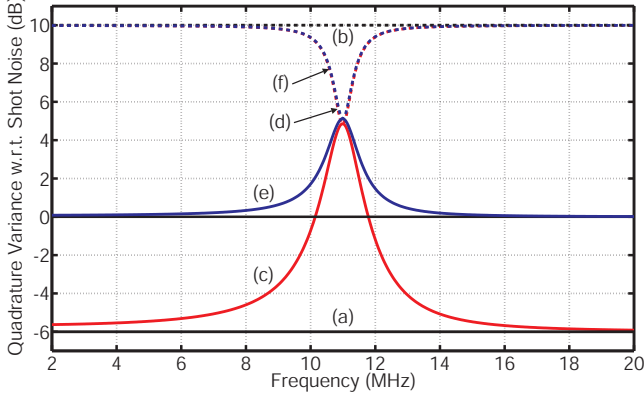


FIG. 2: (Color online) Comparison of signal contrast between squeezed and classical fields injected into an impedance-matched cavity. The quadrature variances V_1^b and V_2^b are shown as solid and dashed curves, respectively, for different input states. (a) and (b) show the (impure) input state with $V_1^a = -6$ dB and $V_2^b = 10$ dB, *in the absence of the cavity*. (c) and (d) show the cavity-coupled response to the squeezed and anti-squeezed vacuum injection, respectively. (e) and (f) show the cavity-coupled response to injection of a classically noisy state with $V_1^a = 0$ dB, $V_2^a = 10$ dB. Comparing (e) and (c), we note that squeezing improves the signal contrast, but the classical noise and the anti-squeezed quadrature behave almost identically [cf. (d) and (f)].

corresponding to the squeezed or anti-squeezed level of -13 dB which is the current experimental limit [19, 20], $\langle N \rangle = 4.53$. Therefore, it is fair to say that the optical influence of ideal squeezed vacuum on cavities is negligible.

Similarly, it is instructive to compare this technique to using a classical state. For simplicity, assuming that the quadrature variance in both quadratures is frequency-independent, we consider the case in which the lower sideband is fully transmitted through an impedance-matched cavity and the upper sideband is fully reflected at the input mirror such that $r_c(-\Omega) = 0$ and $r_c(\Omega) = 1$ at $\Omega = \omega_d$, respectively, which gives $A_+ = A_- = 1/2$ from Eq. (23). Thus, the amplitude and phase quadrature variances of the reflected field are found to be

$$V_1^b(\omega_d) = V_2^b(\omega_d) = \frac{1}{4} (V_1^a + V_2^a) + \frac{1}{2}. \quad (33)$$

In the absence of coherent light, the signal contrast can be defined as the quadrature variance at detuning frequency ω_d compared to the cavity-uncoupled quadrature variance at off-resonance frequencies ($|\Omega - \omega_d| \gg \gamma$), in which case $V_1^b = V_1^a$ and $V_2^b = V_2^a$, and the signal contrasts at the two orthogonal quadratures are respectively given by

$$S_1(\omega_d) = \frac{V_1^b(\omega_d)}{V_1^a} = \frac{\frac{1}{4}(V_1^a + V_2^a) + \frac{1}{2}}{V_1^a}, \quad (34)$$

$$S_2(\omega_d) = \frac{V_2^b(\omega_d)}{V_2^a} = \frac{\frac{1}{4}(V_1^a + V_2^a) + \frac{1}{2}}{V_2^a}. \quad (35)$$

In the limiting case of $V_2^a \gg V_1^a$ and $V_2^a \gg 1$, we obtain

$$S_1(\omega_d) \simeq \frac{V_2^a}{4V_1^a}, \quad (36)$$

$$S_2(\omega_d) \simeq 4. \quad (37)$$

We see that S_2 has about the same limiting level as in the classical case, while S_1 grows if V_1^a gets smaller. Classically, $V_1^a \geq 1$ (the shot noise limit), but using squeezed vacuum we can obtain $V_1^a < 1$, or improved signal contrast for a measurement in the squeezed quadrature. This is illustrated in Fig. 2, where we compare the signal contrast for measurement of the cavity linewidth using a classical field with the signal contrast for squeezed field injection. The cavity-coupled responses of the classical and anti-squeezed quadrature variances behave almost identically in the case of the impedance-matched cavity, whereas squeezing improves the signal contrast of the measurement.

C. Fundamental Limit on Measurement Uncertainty

It is important to note that even in the absence of technical noise, quadrature variance measurements are intrinsically contaminated by quantum noise itself. The standard deviation of the quadrature variances is given by [21]

$$\Delta V_j^b = \sqrt{2} V_j^b \quad \text{for } j = 1, 2. \quad (38)$$

Thus, the noise of the measurement is proportional to the measured value itself, and many averages can be performed to achieve smaller uncertainty levels.

This is different from the classical case where the parameters of a cavity are measured by measuring the transmission of a probe optical field incident on the cavity as a function of cavity detuning. In this case, the measurements are fundamentally limited by shot noise: the number of measured photons (N) has uncertainty proportional to \sqrt{N} . Therefore, the signal-to-noise ratio grows as the number of the transmitted photons increases.

III. EXPERIMENT

The experiment is schematically shown in Fig. 3. The Nd:YAG laser (Lightwave Model 126) gives an output of cw 700 mW at 1064 nm, which is injected into the squeezed vacuum generator (squeezer). The squeezer is composed of a second harmonic generator (SHG) and an optical parametric oscillator (OPO), both using 5% MgO:LiNbO₃ nonlinear crystals placed within optical cavities (hemilith for the SHG and monolith for the OPO) in the Type I phase-matching configuration. The SHG pumped by the Nd:YAG laser generates 250 mW at 532 nm, which then pumps the OPO below threshold

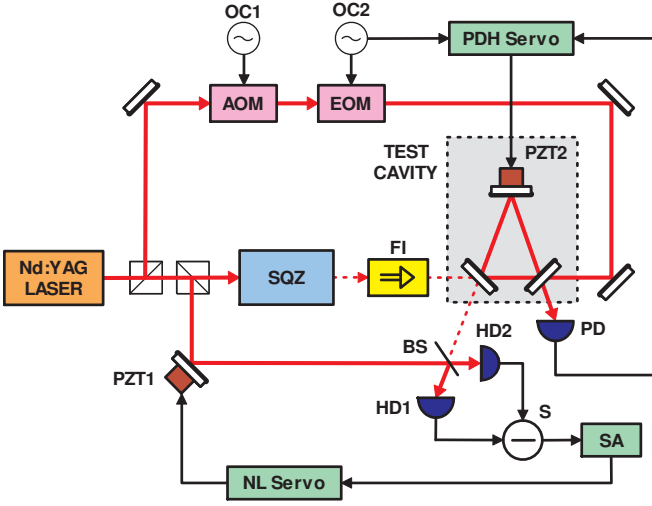


FIG. 3: (Color online) Schematic of the experiment. SQZ: squeezed vacuum generator, FI: Faraday isolator, AOM: acousto-optic modulator, EOM: electro-optic modulator, OC1 and OC2: oscillators, PZT1 and PZT2: piezo-electric transducers, PD: photo-detector, HD1 and HD2: homodyne photo-detectors, BS: 50/50 beamsplitter, S: subtractor, SA: spectrum analyzer, NL Servo: noise-locking servo, PDH Servo: PDH-locking servo. The oscillators (OC1, OC2) are driven at 11.0 ± 0.1 MHz and 13.3 ± 0.1 MHz respectively. The squeezed vacuum generator is composed of an optical parametric oscillator (OPO) and a second harmonic generator (SHG) that pumps the OPO. The cavity length is locked to the laser frequency by the PDH-locking servo and PZT (PZT2). The homodyne angle is locked by the noise-locking servo and PZT (PZT1).

with a vacuum seed. The resultant field generated by the OPO is a squeezed vacuum field with a squeezing bandwidth of 66.2 MHz defined by the OPO cavity linewidth. A sub-carrier field, frequency-shifted by an acousto-optic modulator (AOM) to a frequency that is coincident with the cavity TEM_{01} mode, is injected into the other end of the OPO cavity. The cavity is thus locked to the TEM_{01} mode, offset by 220 MHz from the carrier frequency, using the Pound-Drever-Hall (PDH) locking technique [22]. The frequency-shift is necessary to ensure that no cavity transmitted light at the fundamental frequency is injected into the OPO cavity since it acts as a seed and degrades broadband squeezing due to the imperfect isolation of the Faraday isolator [23, 24]. This is especially important for high Q cavities with linewidths as narrow as kHz because low-frequency squeezing is difficult to achieve.

The squeezed vacuum is injected into a triangular test cavity with the FSR of 713 MHz and FWHM of $\gamma = 856 \pm 34$ kHz, both measured by traditional methods using light. The frequency shift, of the subcarrier is 231 ± 0.1 MHz so that the carrier frequency is detuned from the TEM_{00} mode by 11.0 ± 0.1 MHz. As a result of this frequency shift, only the upper sidebands are within the cavity linewidth, destroying the correlation between

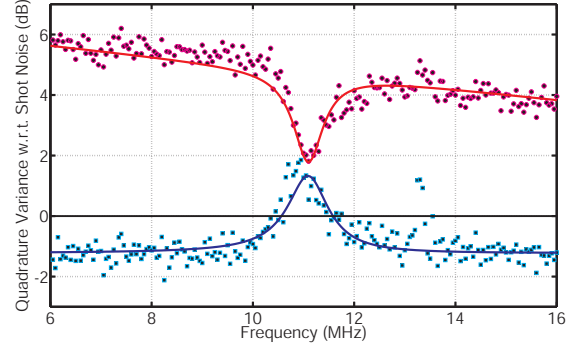


FIG. 4: (Color online) Measured squeezed and anti-squeezed quadrature variances with respect to shot noise (dots) and fits to the data points (curves) using Eq. (27). The resolution bandwidth of the spectrum analyzer is 100 kHz. The data are exponentially averaged 100 times. The apparent peak at 13.3 MHz is due to the coupling of the EOM modulation at the frequency for the PDH-locking technique. The overall decrease in the squeezing and anti-squeezing levels with frequency is due to the OPO cavity linewidth. With the optically measured FSR, the linewidth is found from the fits to be $\gamma = 844 \pm 40$ kHz.

the upper and lower sidebands and, therefore, destroying the squeezing or anti-squeezing. This cavity-coupled squeezed vacuum reflection is measured by balanced homodyne detection, where the field to be measured interferes with a local oscillator (LO) field and is detected by two (nearly) identical photodetectors. The difference of the two photodetector signals is sent to an HP4195A spectrum analyzer (SA) to measure the noise variance of the squeezed or anti-squeezed quadrature. The results are shown in Fig. 4. The experimental data are exponentially averaged 100 times. The resolution bandwidth of the spectrum analyzer is 100 kHz. Since the squeezed vacuum does not carry any coherent amplitude, the noise-locking technique [21] is employed to lock the homodyne angle to either the squeezed or anti-squeezed quadrature at 2 MHz.

Before fitting the experimental data points, the homodyne efficiencies ϵ_{hc} and ϵ_{hm} , and the quantum efficiency of the photo-detectors ϵ_{QE} need to be taken into account. The sum of the homodyne efficiencies and the quantum efficiency were independently measured to be 90% and 85% respectively. The sum of the efficiencies $\eta_c + \eta_m$ in Eq. (27) is given by $\eta_c + \eta_m = (\epsilon_{hc} + \epsilon_{hm})\epsilon_{QE}$. We ignore ϵ_{hm} since the cavity mode-matching efficiency is 82% and hence $\epsilon_{hm} \ll \epsilon_{hc}$, which yields $\eta_l \simeq 1 - \eta_c$. Moreover, we have assumed that the input mirror M_1 is lossless. This assumption is valid since it is a single-pass loss and does not influence the linewidth of the cavity. We then fit Eq. (27) to the measured data points with free parameters R_1, R_2, R_3 , and ω_d ; both the data and the fits are shown in Fig. 4. The resulting fitting values are $\sqrt{R_1 R_2 R_3} = 0.99628 \pm 0.00016$, $\sqrt{R_1} = 0.99783 \pm 0.00005$, and $\omega_d/(2\pi) = 11.098 \pm 0.017$ MHz.

Therefore, the FWHM linewidth of the cavity is found to be $\gamma = 844 \pm 40$ kHz, which agrees with the classically measured linewidth of the cavity within the uncertainty ($\gamma = 856 \pm 34$ kHz). We note that ω_{FSR} can be determined from the fit, but here we have used the optically measured value to estimate the linewidth. This is valid because any loss in the cavity does not change the FSR.

IV. CONCLUSION

We have proposed and experimentally demonstrated a method for non-invasive measurements of optical cavity parameters by use of squeezed vacuum. The technique has the advantage over traditional optical methods that the injection of a squeezed vacuum field as a probe for cavity parameters does not excite any nonlinear processes in cavities, and is, therefore, useful for ultrahigh Q cavities such as whispering gallery mode (WGM) cavities. We have shown that when a squeezed vacuum field

is injected into a detuned cavity, the linewidth and Q factor of a test cavity can be determined by measuring the destruction of upper and lower quantum sidebands with respect to the carrier frequency. The linewidth of a test cavity is measured to be $\gamma = 844 \pm 40$ kHz, which agrees with the classically measured linewidth of the cavity within the uncertainty ($\gamma = 856 \pm 34$ kHz). We have also show that the use of squeezed fields leads to better signal contrast, as expected.

V. ACKNOWLEDGMENTS

We would like to thank our colleagues at the LIGO Laboratory, especially Thomas Corbitt and Christopher Wipf, and Stan Whitcomb for his valuable comments on the manuscript. We gratefully acknowledge support from National Science Foundation Grant Nos. PHY-0107417 and PHY-0457264.

-
- [1] V. S. Ilchenko, A. A. Savchenkov, A. B. Matsko, and L. Maleki, *Phys. Rev. Lett.* **92**, 043903 (pages 4) (2004).
 - [2] K. J. Vahala, *Nature* **424**, 839 (2003).
 - [3] A. A. Savchenkov, V. S. Ilchenko, A. B. Matsko, and L. Maleki, *Phys. Rev. A* **70**, 051804 (2004).
 - [4] M. L. Gorodetsky, A. D. Pryamikov, and V. S. Ilchenko, *J. Opt. Soc. Am. B* **17**, 1051 (2000).
 - [5] A. A. Savchenkov, A. B. Matsko, D. Strekalov, M. Mohageg, V. S. Ilchenko, and L. Maleki, *Phys. Rev. Lett.* **93**, 243905 (2004).
 - [6] A. A. Savchenkov, Private communication (2006).
 - [7] C. M. Caves, *Phys. Rev. D* **23**, 1693 (1981).
 - [8] K. McKenzie, D. A. Shaddock, D. E. McClelland, B. C. Buchler, and P. K. Lam, *Phys. Rev. Lett.* **88**, 231102 (2002).
 - [9] M. Xiao, L.-A. Wu, and H. J. Kimble, *Phys. Rev. Lett.* **59**, 278 (1987).
 - [10] P. Grangier, R. E. Slusher, B. Yurke, and A. LaPorta, *Phys. Rev. Lett.* **59**, 2153 (1987).
 - [11] F. Marin, A. Bramati, V. Jost, and E. Giacobino, *Opt. Comm.* **140**, 146 (1997).
 - [12] A. Furusawa, J. L. Sorensen, S. L. Braunstein, C. A. Fuchs, H. J. Kimble, and E. S. Polzik, *Science* **282**, 706 (1998).
 - [13] C. H. Bennett, F. Bessette, G. Brassard, L. Salvail, and J. Smolin, *J. Crypto.* **5**, 3 (1992).
 - [14] M. I. Kolobov, *Rev. Mod. Phys.* **71**, 1539 (1999).
 - [15] C. M. Caves and B. L. Schumaker, *Phys. Rev. A* **31**, 3068 (1985).
 - [16] B. L. Schumaker and C. M. Caves, *Phys. Rev. A* **31**, 3093 (1985).
 - [17] A. E. Siegman, *Lasers* (University Science Books, 1986).
 - [18] M. O. Scully and M. S. Zubairy, *Quantum Optics* (Cambridge University Press, 1997).
 - [19] P. K. Lam, T. C. Ralph, B. C. Buchler, D. E. McClelland, H.-A. Bachor, and J. Gao, *J. Opt. B: Quantum Semiclass. Opt.* **1**, 469 (1999).
 - [20] T. Aoki, G. Takahashi, and A. Furusawa, *quant-ph/0511239* (2005).
 - [21] K. McKenzie, E. E. Mikhailov, K. Goda, P. K. Lam, N. Grosse, M. B. Gray, N. Mavalvala, and D. E. McClelland, *J. Opt. B: Quantum Semiclass. Opt.* **7**, S421 (2005).
 - [22] R. W. P. Drever, J. L. Hall, F. V. Kowalski, J. Hough, G. M. Ford, A. J. Munley, and H. Ward, *Appl. Phys. B* **31**, 97 (1983).
 - [23] K. McKenzie, N. Grosse, W. P. Bowen, S. E. Whitcomb, M. B. Gray, D. E. McClelland, and P. K. Lam, *Phys. Rev. Lett.* **93**, 161105 (2004).
 - [24] W. P. Bowen, R. Schnabel, N. Treps, H.-A. Bachor, and P. K. Lam, *J. Opt. B: Quantum Semiclass. Opt.* **4**, 421 (2002).